The sine-Gordon Equation in Josephson-Junction Arrays

Juan J. Mazo and Alexey V. Ustinov

Abstract Superconducting Josephson-junctions are excellent experimental systems for the general study of nonlinear phenomena and nonlinear localised excitations. Specifically, a long Josephson-junction is described by the continuous sine-Gordon equation and a Josephson-junction parallel array by its discrete counterpart. This chapter constitute a revision of the physics of such superconducting systems in the light of the sine-Gordon equation.

Keywords Breather • Discrete breather • Flux quantum • Fluxon • Frenkel–Kontorova model • Josephson junction • Josephson junction array • Kink • Long Josephson junction • Quantum solitons • Qubits • Rotobreather • Soliton • Vortex

J.J. Mazo (✉)
Dpto. Física de la Materia Condensada and Instituto de Ciencia de Materiales de Aragón, CSIC-Universidad de Zaragoza, 50009 Zaragoza, Spain
e-mail: juanjo@unizar.es

A.V. Ustinov
Physikalisches Institut, Karlsruhe Institut fuer Technologie, Wolfgang-Gaede str 1, D-76131, Karlsruhe, Germany

National University of Science and Technology MISIS, Leninskiy prospekt 4, 119049 Moscow, Russian Federation

Russian Quantum Center, Novaya str., 100, BC "URAL", SKOLKOVO, Moscow region, 143025 Russian Federation
e-mail: ustinov@kit.edu

J. Cuevas-Maraver et al. (eds.), *The sine-Gordon Model and its Applications*, Nonlinear Systems and Complexity 10, DOI 10.1007/978-3-319-06722-3_7,

1 Introduction

The concept of coherent structures or coherent excitations has important consequences when applied to condensed matter systems. Spatially or temporally coherent structures appear in many nonlinear extended systems. Such structures usually can be characterized by marked particle-like properties. In the past few years, these notions have become fundamental for understanding many problems and their implications extend over different fields of the physics of continuous and discrete systems [1, 2].

Josephson-junction (JJ) arrays are a very good example of a physical system where such type of structures appear. In particular, long Josephson-junctions (LJJs) are paradigmatic devices to study soliton dynamics. This article is a personal, partial and subjective introduction to the physics of this system and its discrete counterpart. They have been widely studied in the past. Authoritative reviews on the subject can be found in [3–8].

We will introduce first the main aspects of the physics of superconducting JJs to present simple model descriptions of long Josephson arrays. We will revise the most prominent fluxon dynamics results in man-made and natural systems. Then, we will move to the discrete version of the long junction: a set of parallelly connected small JJs. We will finish with results on quantum dynamics of solitons in long JJs, and a few words about future perspectives.

2 Superconducting Josephson Effect

2.1 Josephson Effect

In his pioneering work of 1962 Brian Josephson studied the tunnel of Cooper pairs between superconducting metals and predicted the celebrated Josephson effect [9]; that is, the presence of a supercurrent between two superconductors coupled by a weak link, an artifice known as a Josephson junction. Since then, many works have been done which study the behavior of single junctions, JJ arrays, and other more complex devices with Josephson elements, and their outstanding applications [5, 10–13].

2.2 Superconducting Tunnel Junctions

A Josephson tunnel junction is a solid state physics device which consist of two superconducting electrodes (usually Niobium or Aluminum) separated by a thin insulating barrier (usually an Aluminum oxide), see Fig. 1.

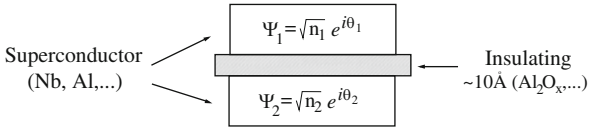

Fig. 1 Schematic diagram of a Josephson tunnel junction: two superconducting electrodes separated by a thin insulating barrier

The physics of the junction is given by the value of the gauge invariant phase difference between the superconducting electrodes $\varphi = \theta_1 - \theta_2 - \frac{2e}{\hbar}\int_1^2 \boldsymbol{A}(\boldsymbol{r},t)\,\boldsymbol{dl}$, with θ_i the phase of the macroscopic wave function in electrode i ($\Psi_i = \sqrt{n_i}e^{i\theta_i}$) and $\boldsymbol{A}$ the vector potential.

The basic equations for the Josephson effect are

$$I_s = I_c \sin\varphi \tag{1}$$

and

$$V = \frac{\hbar}{2e}\frac{d\varphi}{dt}. \tag{2}$$

They establish—*DC Josephson effect*—that at zero voltage (then φ is constant) it is possible to have a dc current across the junction. The maximum possible value of this current is I_c, the junction critical current. However—*AC Josephson effect*—in the presence of a constant voltage the junction responses with an ac current of frequency $2eV/\hbar$ (483.6 GHz for a typical value of 1 mV). Note that the $\hbar/2e$ quotient can be also written in terms of the flux quantum unit $\Phi_0 = h/2e$. Thus $\hbar/2e = \Phi_0/2\pi$.

The most important characteristic curve of the junction is the current-voltage ($I-V$) one, which measures the response, voltage, of the junction to an injected current. This can be modeled in its simplest version by the RCSJ (resistively and capacitively shunted junction) model [14, 15] (see Fig. 2). In this model the total current through the junction is the sum of three contributions: the Josephson supercurrent, a resistive normal current (tunneling of normal carriers from one electrode to the other) and a capacitive channel (associated with the junction capacitance); $I = I_J + I_R + I_C$ with $I_J = I_c \sin\varphi$, $I_R = V/R$ and $I_C = C\,dV/dt$. Then

$$I = C\dot{V} + \frac{1}{R}V + I_c \sin\varphi. \tag{3}$$

If we apply the second Josephson relation and normalize current with respect to the junction critical current, $i = I/I_c$, time with respect to the Josephson

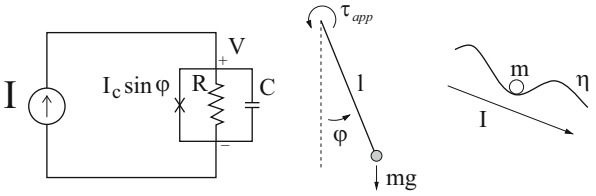

Fig. 2 RCSJ circuit model of the junction and two mechanical analogs: the forced and damped pendulum and the particle in the tilted washboard potential

plasma frequency $\omega_p = \sqrt{2\pi I_c/\Phi_0 C}$ and introduce the damping parameter $\Gamma = \sqrt{\Phi_0/2\pi I_c C R^2}$,[1] we obtain

$$i = \mathcal{N}(\varphi) = \ddot{\varphi} + \Gamma\dot{\varphi} + \sin\varphi. \tag{4}$$

This is the normalized equation for the dynamics of a single junction biased by an external current. This equation is identical to the equation for a forced and damped pendulum in a gravitational field or a particle in a tilted washboard potential $U(\varphi) = -E_J\cos\varphi - (\hbar I/2e)\varphi$ [mass $m = (\hbar/2e)^2 C$ and damping $\gamma = (\hbar/2e)^2(1/R)$], see Fig. 2. Both are simple mechanical analogs for the junction and illustrate that JJ devices are ideal experimental systems to probe basic nonlinear science results.

Thermal fluctuations can be included in the model by the addition of a noise current source $\tilde{I}(t)$ with $\langle\tilde{I}(t)\rangle = 0$ and $\langle\tilde{I}(t)\tilde{I}(t')\rangle = (2k_BT/R)\delta(t-t')$. In this case, the total current, in normalized units, is

$$i = \mathcal{N}(\varphi) = \ddot{\varphi} + \Gamma\dot{\varphi} + \sin\varphi + \tilde{\imath} \tag{5}$$

with $\langle\tilde{\imath}(\tau)\rangle = 0$ and $\langle\tilde{\imath}(\tau)\tilde{\imath}(\tau')\rangle = (2\Gamma k_BT/E_J)\delta(\tau-\tau')$.

3 Long Josephson Junctions

3.1 The Long JJ and the sine-Gordon Equation

A long Josephson junction (Fig. 3) is a junction which has one dimension (say x) long with respect to the so called Josephson penetration depth, λ_J [5], see below. Then, the phase difference is also a function of the spatial coordinate: $\varphi(x,t)$.

[1] The damping can be also defined in terms of the so-called quality factor $Q = 1/\Gamma$ or the Stewart-McCumber parameter $\beta_c = 1/\sqrt{\Gamma} = 2\pi I_c CR^2/\Phi_0$.

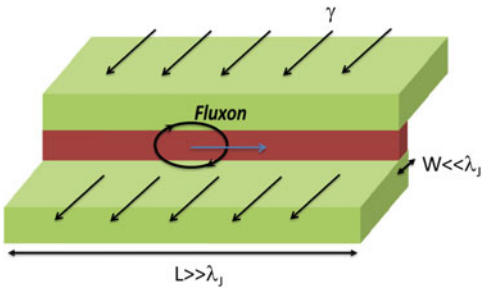

Fig. 3 Schematic diagram of a long JJ with a fluxon (also know as Josephson vortex) driven by an external current γ

Accordingly we introduce an spatial dependence in current and voltage along the junction, $V(x)$ and $I(x)$, which neglecting dissipative effects change as:

$$\begin{aligned} \frac{\partial V}{\partial x} &= -L\frac{\partial I}{\partial t} \\ \frac{\partial I}{\partial x} &= -C\frac{\partial V}{\partial t} - I_c \sin\varphi \end{aligned} \tag{6}$$

Here, L and C are respectively the inductance and capacitance per unit of length of the junction.

Introducing the Josephson relations, we see that in its simplest approach the electrodynamics of the junction is described by the following sine-Gordon equation:

$$\lambda_J^2 \frac{\partial^2\varphi}{\partial x^2} - \frac{1}{\omega_p^2}\frac{\partial^2\varphi}{\partial t^2} = \sin\varphi. \tag{7}$$

Here $\lambda_J = \sqrt{\Phi_0/2\pi L I_c}$ is the *Josephson penetration depth* and $\omega_p = \sqrt{2\pi I_c/\Phi_0 C}$ the *Josephson plasma frequency* of the system, which give a measure of the natural length and time units. Measuring length in units of λ_J and time in units of ω_p^{-1} we get the dimensionless equation for the system,

$$\varphi_{xx} - \varphi_{tt} = \sin\varphi \tag{8}$$

When losses and bias are included the dynamics of the phase is described by the perturbed sine-Gordon equation [16]

$$\varphi_{xx} - \varphi_{tt} - \sin\varphi = \alpha\varphi_t - \beta\varphi_{xxt} - \gamma. \tag{9}$$

α measures the intensity of a dissipative term due to quasi-particle tunneling through the junction, β measures the surface resistance of the superconductors and γ the normalized bias current.

Fig. 4 Different geometries for a long JJ: overlap junction (*left*); in-line junction (*middle*); and annular junction (*right*)

3.2 Geometries for Long JJs

In any real system, the perturbed sine-Gordon equation (9) has to be solved together with appropriate boundary conditions. These conditions depend on the specific junction geometry. By *long* Josephson junction, we simply mean that the Josephson phase difference can vary along only one of its spatial dimensions, let's say the x-coordinate. We distinguish between such long junctions and short junctions (as presented in Sect. 2.2), for which the phase difference is (nearly) constant over the whole junction area.

Thus, for a long JJ we need: (1) a junction length $L \gg \lambda_J$ (φ changes along this direction); (2) a junction width $W \ll \lambda_J$ (φ nearly constant along this direction); and (3) the external magnetic field H applied perpendicular to the junction (a non-zero parallel component induces phase difference variations along the perpendicular direction).

Such quasi-one-dimensional Josephson junctions can be constructed in different ways, and junction geometry has a significant effect on soliton dynamics. The most extensively studied variations are the overlap geometry, the in-line geometry and the annular geometry, depicted in Fig. 4. They are studied by a perturbed sine-Gordon equation with appropriate boundary conditions.

In the more general case we deal with *large* (in both x and y dimensions) junctions, which are described by a partial differential equation (PDE) in two space dimensions, x and y, and time t: a 2d sine-Gordon equation.

3.3 Fluxons in Long JJs

The soliton solution of the sine-Gordon solution has a well defined physical meaning in the context of the long JJ systems, since it corresponds to a quantum of flux trapped in the junction. Thus, the soliton is usually referred to as *fluxon* or *Josephson vortex* in the context of long JJ.

Figure 5 schematically shows the fluxon in the array. It corresponds to a solution of the phase changing from 0 to 2π along the junction. The width scale for the change of the phase, the width of the fluxon, is given by the Josephson penetration depth λ_J. A spatial variation of the phase gives account of a magnetic flux in the system, as depicted in the figure, whose total integral is equal to one flux

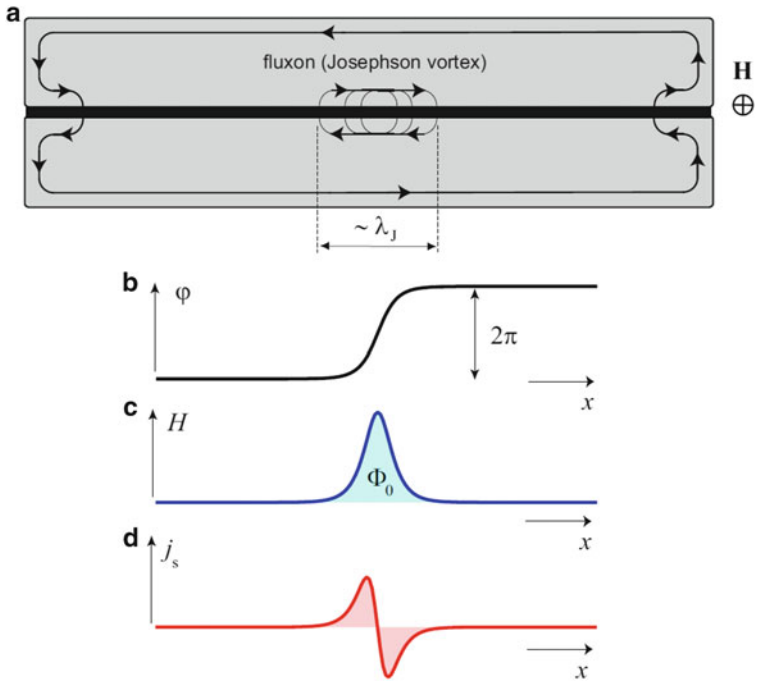

Fig. 5 (**a**) Schematic diagram of a long JJ with a fluxon in it and (**b**) phase φ, (**c**) field $H \sim \partial\varphi/\partial x$ and (**d**) density of superconducting current $j_s \sim \sin\varphi$ for a soliton in the junction. The fluxon extends over a physical distance of the order of λ_J

quantum Φ_0. In addition, from the Josephson relations we know that a non zero phase variation corresponds to a flowing supercurrent which, as shown in the figure, circulates around the fluxon core.

Similarly to single fluxons, the system also supports for multifluxon solutions formed by a set of fluxon, or antifluxons, or combinations of both.

3.4 Dynamical Solutions of Unperturbed Long JJs

In addition to static solutions ($\varphi = 0$ and fluxons), the unperturbed sine-Gordon equation, Eq. (8), also supports a family of dynamical solutions, mainly moving fluxons, small-amplitude waves and breathers.

Small-amplitude waves, $\varphi \ll 2\pi$, are obtained by taking the linear limit of the sinusoidal term in Eq. (8). The resulting equation has plane wave solutions

$$\varphi \sim e^{i(kx-\omega t)} \tag{10}$$

with $\omega^2 = 1 + k^2$ (we have previously normalized by ω_p and λ_J). This dispersion relation is linear at large k and shows a forbidden gap for small frequencies.

Fluxons solutions appear as static or moving solutions of the system. They are given by

$$\varphi = 4 \arctan \left[\exp \left(\pm \frac{x - vt - x_0}{\sqrt{1 - v^2}} \right) \right]. \tag{11}$$

The sign stands for fluxon or anti-fluxon solutions where the phase goes from 0 to $+2\pi$ or -2π respectively. Moving fluxons travel at constant velocity v without change in its shape.

Breather solutions are periodic oscillating localized solutions of the system without a topological charge. They can be depicted as a bound soliton-antisoliton pair and exist also as moving solutions along the junction.

4 Fluxon Dynamics in Long Josephson Junctions

4.1 Fluxon Dynamics

We have previously introduced the perturbed sine-Gordon equation, Eq. (9), describing a long quasi-one-dimensional Josephson junction and reviewed in Sect. 3.4 the most important exact solutions of the unperturbed sine-Gordon equation. Since the perturbation terms are usually small, one might think that the reviewed solutions would remain almost unchanged, or would acquire small corrections. To a large extent, this thinking is correct. Soliton and antisoliton solutions for the sine-Gordon equation are only slightly modified in a real junction. In contrast, breather solutions and isolated plasma wave packets do not survive dissipative perturbations, and decay with time. Though these solutions can be excited, e.g., by current pulses, they exist in real junctions only for very short times (in physical time units, several nanoseconds).

There exist several ways of addressing Eq. (9), for which there are not known analytical solutions. A first possibility is to perform a perturbative analysis, starting form the unperturbed sine-Gordon equation. The perturbation theory for solitons in Josephson junctions was put together in the classic paper by McLaughlin and Scott, published in 1978 [4]. Another perturbative analysis can be found in [17].

A standard tool of Josephson junction analysis is the energy balance approach. It allows for predicting the velocity v of a steadily moving soliton driven by a current γ balanced by the power loss due to the dissipative terms α and β,

$$\gamma = \frac{4}{\pi} \frac{v}{\sqrt{1 - v^2}} \left[\alpha + \frac{\beta}{3(1 - v^2)} \right] \tag{12}$$

The velocity predicted by Eq. (12) is in good agreement with direct numerical simulations of the perturbed sine-Gordon equation, Eq. (9). The soliton behaves

in much the same way as does a relativistic particle having a normalized limiting velocity equal to unity. Similar expressions have been derived for the velocity of a soliton train propagating in the array.

In an experiment, α and β are usually fixed by the intrinsic properties of a given Josephson junction and by the temperature whereas γ is proportional to the bias current and, consequently, it can be easily varied in an experiment. Thus Eq. (12) determines the *current-voltage characteristics* of the system, the curve usually measured by experiments. Experimental curves can be almost perfectly fitted to the analytical power-balance equation (9).

There exist no infinite real junctions. Thus the dynamics of fluxons in long Josephson junctions depends importantly on the geometry and boundaries of the junction. The case of annular junctions is the simplest one, as traveling solitons (or antisolitons) will move interacting with the electromagnetic waves generated in its circular trajectory. For open junctions at zero magnetic field, the border behaves as a mirror and a soliton reaching the boundary is reflected as an antisoliton moving in the opposite direction. The soliton collision process with an open boundary can be viewed as a *virtual collision with an antisoliton*. There exists, however, a minimum soliton velocity below which a soliton and an antisoliton will not survive a collision. This minimum allows to define a minimum bias current for observing vortex reflection at the junction boundary. This simple picture is importantly modified by the presence of magnetic fields which affect the boundary conditions of the junction.

Characteristic curves of long Josephson-junctions typically show a series of branches, called *zero field steps*, associated to the dynamics of a number of solitons and antisolitons moving in the junction. First experimental indications of the magnetic flux motion in Josephson junctions date back to 1969 [18–20]. Soon after that, in 1972, Fulton and Dynes [21] performed a pioneering experiment with a long Josephson junction and clearly interpreted their data as due to the inertial motion of fluxons in the junction and named the resonant structures observed in the current-voltage characteristic of the junction as *zero-field steps*. Zero-field steps are related to the resonant oscillations of fluxons trapped in the long Josephson junction in the absence of an external field (see Fig. 6).

4.2 Annular Junctions and Fluxon Pinning Potential

Annular junctions are ideal systems for studying fluxon dynamics since they allow to observe undisturbed fluxon motion. Single sine-Gordon solitons trapped in an annular Josephson junction were observed for the first time by Davidson et al. [22, 23]. Particularly interesting, fluxon and antifluxons can be introduced at will in the systems, permitting to study fluxon dynamics in a very controlled way [24, 25]. In addition to the usual curves, experiments indicating the excitation

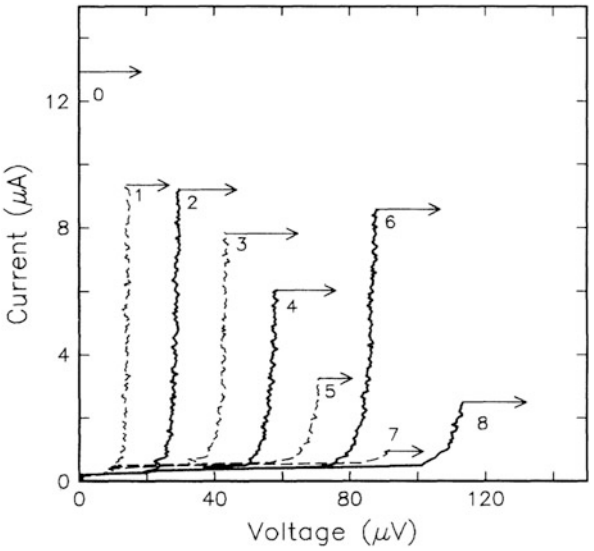

Fig. 6 Zero field steps appear in the current vs. voltage curve of a LJJ. Each number gives the total number of solitons and antisolitons moving in the junction. Reprinted figure with permission from A. Davidson, B. Dueholm, B. Kryger, and N. F. Pedersen, Physical Review Letters 55, 2059 (1985). Copyright 1985 by the American Physical Society

of electromagnetic modes by a vortex moving in an annular Josephson junction were reported [26]. Such modes were visible as resonances on the current-voltage characteristic of the junction.

In 1991 Grønbech-Jensen et al. [27] proposed a model for an annular Josephson junction in an external magnetic field. They showed that the field introduces an additional term in the perturbed sine-Gordon equation which describes the system. This extra term accounts for the coupling between the applied field and the flux density in the junction inducing a pinning potential for the fluxon. The static properties of the system were experimentally studied in [28] and the dynamical behavior of the fluxon in [29]. It was shown that, in the presence of a periodic pinning potential, the behavior of the fluxon in the LJJ is very similar to the response of a small junction; the fluxon can be seen as a single particle moving in a washboard potential. Thermal activation properties of the fluxon over the barrier were studied in [30]. There, a most interesting topic was discussed: the possibility of realizing fluxon potential engineering. In particular, a heart-shaped junction resulting in a double-well was shown. We will go discuss again this system in the last section when introducing quantum solitons in LJJs.

Shape engineering of closed LJJs allowed also for the proposal of a Josephson vortex ratchet [31]. In such system a Josephson vortex moves in a periodic asymmetric potential. Soon after, Carapella and Costabile [32] reported the observation of the ratchet effect for a fluxon trapped in an annular Josephson junction embedded in an inhomogeneous magnetic field. In [33] the ratchet effect is also experimentally studied, but in that case the asymmetric potential was caused by a current injector. Similar effects were studied later on in intrinsic BSCCO JJs [34].

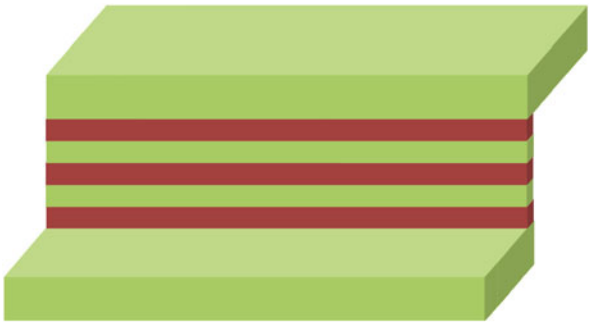

Fig. 7 Example of series of stacked LJJs

5 Stacked Josephson Junctions

A new superconducting system that is described by special fluxon solutions is the long stacked Josephson junction sketched in Fig. 7 which consists of a series of alternating superconducting and isolating layers [8]. This type of systems can be studied in terms of N inductively coupled perturbed sine-Gordon equations [35] where the coupling is due to induced currents in superconducting regions shared by fluxons belonging to different layers.

Fluxons in coupled LJJs have been a subject of intensive theoretical and experimental investigation [8]. On the one side, man-made stacked LJJs with very few layers are interesting from a fundamental point of view [36–39]. In a magnetic field applied parallelly to the layers, fluxons are expected to penetrate into different Josephson junctions and may move coherently due to the interaction of their screening currents.

On the other hand, the discovery of the intrinsic Josephson effect in some high-temperature superconductors such as $Ba_2Sr_2CaCu_2O_{8+y}$ (BSCCO) convincingly showed that those materials are essentially natural superlattices of Josephson junctions formed on atomic structure scale [40–42]. The spatial period of such a superlattice is only 15 Å, so the Josephson junctions are extremely densely packed. The superconducting electrodes are formed by the copper oxide bilayers as thin as 3 Å and are separated by the non-superconducting BiO layers. Josephson superlattices with many active layers can naturally be expected to show very complex dynamics. Single crystals of BSCCO and some other materials show properties expected for multi-layer stacks of Josephson junctions [43–46]. Since it is rather difficult to measure the voltage on a single Josephson junction of atomic scale, natural stacks are usually measured in series.

In the last years most attention has been put in these systems triggered by the interest in generating and detecting electromagnetic fields in the elusive low terahertz range, where there is a severe lack of working devices. In particular, solid-state sources of terahertz (THz) radiation are being sought for sensing, imaging, and spectroscopy applications across the physical and biological sciences.

Millimeter-wave oscillators using intrinsic Josephson effect materials go up to sub-THz and THz frequencies and are promising devices for various sub-millimeter band applications [47–54].

6 Josephson Junction Parallel Arrays and the Discrete sine-Gordon Equation

6.1 Parallel Arrays

Systems with superconducting wires interrupted by *small* JJs are usually denoted as JJ arrays [55]. Fabrication techniques nowadays allow to make arrays of many sizes and geometries. Such systems have been extensively studied in the past from both basic and applied perspectives. For instance, series arrays have been designed for studying phase locking phenomena and building the voltage standard [56]. Superconducting loops interrupted by one or two junctions, known as SQUIDs (for *Superconducting Quantum Interference Devices*) [5, 11, 57–59], provide a sensitive measure of magnetic flux and are used nowadays as standard magnetic field detector in many laboratories. Ladder arrays were designed for studying the transition from one-dimensional to two-dimensional physics and allowed an experimental observation of discrete breathers [60, 61]. Two dimensional arrays are an ideal model system to study 2D phase transitions, frustration and disorder effects, vortex dynamics, phase synchronization and other non-linear dynamics results [62]. To finish, the JJ parallel arrays, which had been designed for studying fluxon transport devices, are also interesting from a fundamental point of view as they constitute an experimental realization of the discrete sine-Gordon equation [63–67].

A JJ parallel array is formed by a set of junctions connected in parallel by superconducting wires (as seen in Fig. 8). The equations for the array can be easily obtained when only mesh self-inductances are taking into account [55, 67]. In this case we get:

$$\ddot{\varphi}_j + \Gamma\dot{\varphi}_j + \sin\varphi_j = \lambda\left(\varphi_{j+1} - 2\varphi_j + \varphi_{j-1}\right) + i_{\text{ext}} \tag{13}$$

with $j = 1, \ldots N$. Equation (13) has to be complemented by the appropriate boundary conditions. They are given by $\varphi_0 = \varphi_1 - 2\pi f_0$ and $\varphi_{N+1} = \varphi_N + 2\pi f_0$ for the case of open-ended arrays or $\varphi_{N+1} = \varphi_1 + 2\pi n_k$ and $\varphi_0 = \varphi_N - 2\pi n_k$ for ring arrays. In this last case the integer n_k gives the total number of kinks or fluxons trapped in the array.

It is easy to see that Eq. (13) constitutes the discrete version of the sine-Gordon equation. Let us denote $\varphi_j \equiv \varphi(x)$ and $\varphi_{j\pm1} \equiv \varphi(x \pm \delta)$. For large λ we can write $\varphi(x \pm \delta) \simeq \varphi(x) + \varphi_x\delta \pm \frac{1}{2}\varphi_{xx}\delta^2$ and then $\varphi_{j+1} - 2\varphi_j + \varphi_{j-1} \equiv \varphi_{xx}\delta^2$. Thus λ acts as a discreteness parameter: for large λ the physics of the array corresponds to that of the long JJ meanwhile for moderate and small λ values new discreteness effects appear in the dynamics of the system.

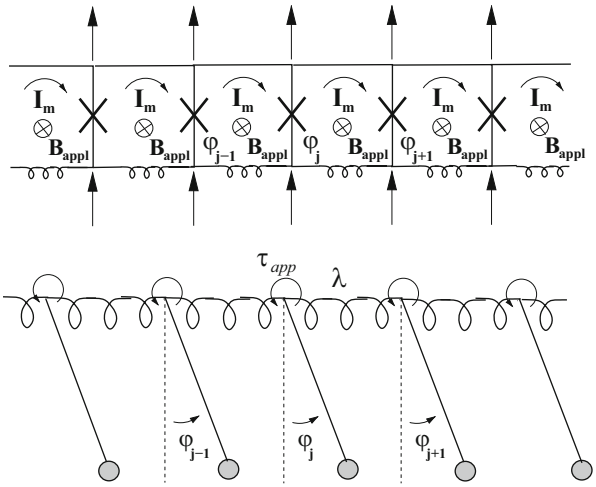

Fig. 8 JJ parallel array and its mechanical analog

Being the pendulum a mechanical analog of the single junction, the mechanical analog of the parallel array is a set of pendula connected by torsion springs (see Fig. 8), or a set of atoms in a periodic substrate potential interacting harmonically; a classical model in condensed matter physics coined under the name of Frenkel–Kontorova model [63–65].

6.2 Kinks in Parallel Arrays

A kink (anti-kink) corresponds to a solution where the phases go from 0 to 2π (-2π) along the array (see Fig. 9). They are the discrete counterpart of the continuous solitons found in the long Josephson-junction.

The existence of kinks does not depend crucially on the discreteness of the system and in many aspects the discrete solitons are similar to the continuous solitons found in the sine-Gordon equation. However, many other properties of the kinks do depend crucially on the discreteness of the array. The existence of a discrete lattice breaks the invariance under continuous translations of the solitons of the continuous model and discrete fluxons are pinned to the lattice: there exists a minimum energy barrier the kink needs to overcome in order to move through the lattice. This energy is the so-called Peierls–Nabarro (PN) barrier, E_{PN}, and decreases rapidly with λ, see [55].

We can go further and define not only a PN barrier but also a center of mass position for the kink ($X = C \pm \sum_j \varphi_j$) and a PN potential. Following this approach it is possible to identify the kink motion with the motion of a single particle over a

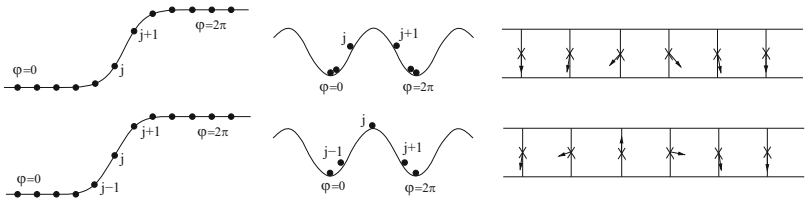

Fig. 9 Three different representations of the minimum energy configuration (*top figures*) and the saddle configuration, maximum of the PN potential (*bottom figures*), of a kink in the parallel array: phase representation (*left*), potential energy representation (*center*) and angular representation (*right*)

sinusoidal periodic potential. In the presence of external bias, an effective equation of motion for the kink is given by

$$m\ddot{X} + m\Gamma\dot{X} + \frac{E_{PN}}{2}\sin X = i. \tag{14}$$

The picture of the kink or fluxon as a single particle is particularly useful in arrays which are larger than the fluxon width and are driven by small currents (far from the whirling mode where all the junctions are in the voltage state and the fluxon delocalizes).

As for the continuous case, when the kink moves it radiates energy in form of small amplitude waves. This radiation is very strong for the case of underdamped arrays. There, phonons are easily excited by the kink in its wake and resonances between the kink velocity and these waves appear [66, 67]. The dispersion relation for such waves can be easily obtained as (for zero damping and current)

$$\omega_k^2 = 1 + 4\lambda \sin^2(k/2) \quad (-\pi < k \leq \pi). \tag{15}$$

Differently from the continuous case, this dispersion relation is characterized by a finite band with gap $\omega_{min} = \omega_0 = 1$ and maximum frequency $\omega_{max} = \omega_\pi = (1 + 4\lambda)^{1/2}$.

Fluxon ratchet potentials. We have considered arrays where all the junctions are identical and all the cells have the same size. However, it is possible to design different arrays which are adequate for studying new physical problems. One example is the use of Josephson parallel arrays to study the dynamics of kinks subjected to substrate ratchet potentials [68–70].

A ratchet potential is a periodic potential without inversion symmetry: $V(x) \neq V(-x)$; then it is easier to move a particle in one direction than in the other. A kink ratchet potential can be obtained with different suitable combinations of junctions and inductances. The simplest ones (see Fig. 10) are made alternating junctions of two critical currents and cells of two areas, and alternating junctions of three critical currents.

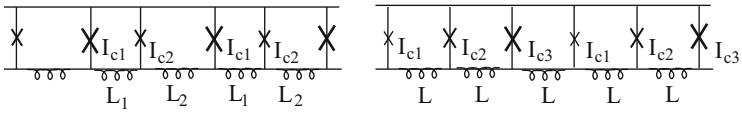

Fig. 10 Two different designs of parallel arrays where fluxons experiment a ratchet periodic potential

4π kinks. To finish, we mention that 4π kinks have been recently observed in the dynamics of Josephson parallel arrays [71]. A 4π kink carries two quanta of magnetic flux and results from the fusion of two standard 2π kinks.

6.3 Discrete Breathers in Parallel Arrays

Discrete breather [72–75] excitations (also called intrinsic localized modes) are solutions of the dynamics of nonlinear lattices for which the energy remains exponentially localized in a few sites of the array. As we have seen, Josephson arrays are ideal experimental discrete system to study nonlinear dynamics. Thus much effort in the last years has been devoted to the prediction and experimental observation of discrete breathers in Josephson arrays.

Josephson circuits are externally biased dissipative systems. Thus, the breather solutions that we are going to present are attractors of the dynamics of the array. The simplest Josephson array supporting breathers is the parallel array, which is described by a discrete sine-Gordon equation. This system supports only oscillobreather solutions where one junction describes a large amplitude oscillation meanwhile the others follow the external force and oscillate with a small amplitude. They appear in arrays biased by ac external currents. Figure 11 shows a picture of an oscillating discrete breather solution in a Josephson parallel array. Being the plasma frequency for a Josephson junction close to 100 GHz, it is not possible to follow the instantaneous dynamics of the phases of the system. The detection of oscillobreathers in parallel arrays is a formidable task which has not been made up to the date. Thus, the experimental effort and much of the theoretical studies of breather in Josephson arrays have been focused to study breathers (rotobreathers) in a variation of the parallel array: the so-called Josephson junction ladder [60, 61, 76, 77]. Different from oscillobreathers, in the rotobreather case one junction is set at the gap-voltage state (following the pendulum analog, it rotates at a given frequency) with the other junctions at zero dc voltage (oscillates with an exponentially decaying amplitude measured from the breather core).

Fluxons and breathers can coexist in ac-biased JJ parallel arrays. Their combined dynamics shows a rich phenomenology depending on the different parameter and conditions of the system. Figure 11 for instance, shows a situation were a fluxon is

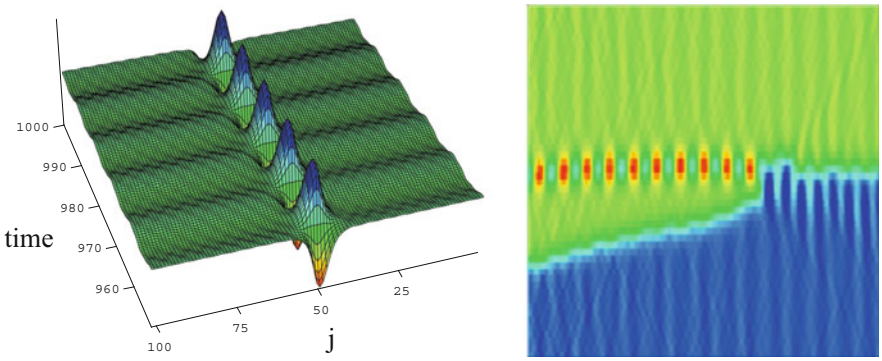

Fig. 11 *Left*: Numerical simulation of a breather solution in an ac biased Josephson parallel array. *Right*: Fluxon breather collision in an ac biased Josephson parallel array

attracted by a oscillobreather. After the interaction the discrete breather excitation is annihilated. Vortex-breather collisions in Josephson ladders were numerically studied in [78].

7 Quantum Solitons in LJJs

Being the Josephson effect a genuine quantum mechanical phenomena, in order to model and understand the behavior of the Josephson arrays previously considered, junctions have been treated as classical elements and Josephson arrays as classical circuits. This approximation, however, ceases to be valid for small enough junctions and at very low temperatures. In such cases, *secondary* quantum effects emerge in the system, and the phase of the junction requires to be treated as a true quantum operator. In such junctions, the phase difference across the junction and the charge on the junction electrode behave as quantum-mechanical conjugate variables. In the case of small junctions the Hamiltonian of the JJ can be written as the addition of Josephson and charging energies

$$H = -E_J \cos\varphi + \frac{Q^2}{2C} \tag{16}$$

where $Q \sim d\varphi/dt$ (that is, the charging energy is a kinetic energy term).

First experimental evidences of quantum mechanical behavior of small JJs were reported in the late 1980s and 1990s [79]. Recently Josephson arrays with small junctions are the base of many promising new quantum technologies [80] for on-chip quantum optics and quantum information processing (recent reviews on the subject are available in [81–83]).

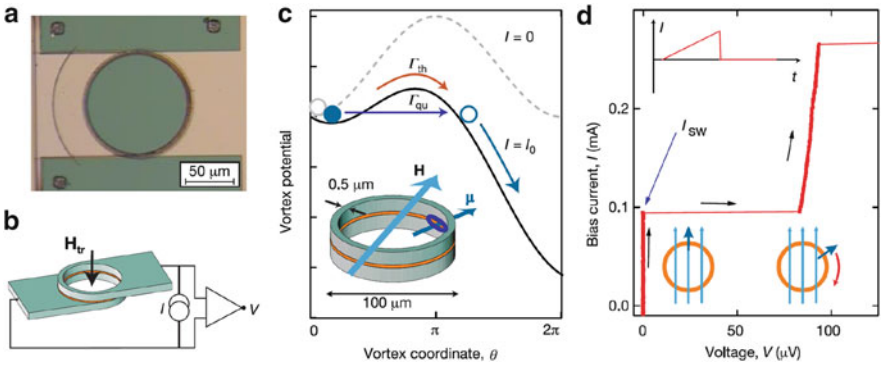

Fig. 12 *Left*: Circular array to explore vortex dynamics. *Middle*: A vortex can escape from a metastable potential due to thermal excitation or to quantum tunneling through a potential barrier. *Right*: Typical current-voltage curve. Switching is due to thermal excitation at high temperatures and to vortex tunneling below a certain temperature crossover [84]

We have shown above that annular junctions are ideal systems for studying Josephson vortices, which in turn behave in many respects as relativistic particles. Such particle should exhibit quantum mechanical properties if studied in suitable arrays and at low temperatures. This study was done by A. Wallraff et al. 10 years ago [84]. They proved the quantum dynamics of an individual Josephson vortex in a long Josephson junction. By measuring the statistics of the vortex escape from a controllable pinning potential, they demonstrated the existence of quantized levels of the vortex energy within the trapping potential well and quantum tunnelling of the vortex through the pinning barrier with a crossover from thermal activation to the macroscopic quantum tunneling observed at about 100 mK, see Fig. 12. In a different work, the thermal and the quantum dissociation of a single vortex-antivortex (VAV) pair in an annular Josephson junction was also experimentally observed [85].

The flexibility in the fabrication of Josephson arrays and the detection of the fluxon quantum tunneling allows to design qubit systems in LJJs. Heart-shaped junctions [30] or annular junction with a microshort [86] shows a double well potential structure for the fluxon; allowing for single vortex tunneling between both states and quantum superposition. The use of circuits based in LJJs for fluxon readout of superconducting qubit has been also recently achieved [87, 88].

8 Final Remarks

We have presented here a short introduction to the physics of long Josephson junctions. Measured for the first time more than 40 years ago, LJJs systems are still nowadays an active research field. Work today is mainly devoted to

the applications of the arrays in two very different fields: developing terahertz technologies and quantum information theory. Substantial advances in both fields are rapidly occurring and foreseeably will occur in the next future.

This chapter has been devoted to *standard* Josephson junctions characterized by the Josephson relation given in Eq. (1). So-called π junctions, characterized by a different Josephson relation ($\varphi = \pi$ instead of 0 in its ground state) are today an important field of research. Then, long π Josephson junctions and combined 0-π junctions, where *fractional vortices* are found, are being proposed and studied with new interesting physics and potential applications in many diverse fields [89–95].

The discrete sine-Gordon model is at the basis for employing magnetic flux quanta in parallel arrays, often referred as Josephson Transmission Lines (JTLs), as basic bits for computation elements. A magnetic flux quantum, or fluxon (2.07×10^{-15} Wb), is alias of a Josephson vortex as it is formed by persistent current loops circulating around a certain point of the superconducting transmission line with embedded Josephson junctions. As discussed earlier in this review, Josephson fluxons behave as particle-like solitary waves—solitons. The idea of using Josephson flux quanta as elementary bits of information goes back to Fulton, Dynes and Anderson [96]. Since two decades ago, fluxons have been successfully employed for the implementation of Rapid Single Flux Quanta (RSFQ) logic in superconducting digital circuits [97–99] using shunted (overdamped) Josephson junctions. The fact that a single flux quantum can be manipulated, moved around by bias currents, erased by magnetic fields etc., stimulates very naturally the variety of ideas and conjectures related to elementary digital operations. More recent ideas involve underdamped dynamics of fluxons in discrete JTLs (alias of parallel arrays discussed earlier in this chapter), which have been proposed to be used for reversible computing [100]. This kind of computing dissipating less than the thermodynamic threshold $k_B T \ln 2$ energy per elementary operation can be performed in either classical or quantum regime [101]. Here fluxons are modified to create an internal degree of freedom with two stable states, which is possible by replacing the elementary Josephson junctions in the JTL by so-called nSQUID elements [102]. A recent historical review on fluxon logic circuits can be found in [103].

Acknowledgements JJM acknowledge financial support from Spanish MINECO through Project No. FIS2011-25167, cofinanced by FEDER funds.

References

1. A. Scott, *Nonlinear Science: Emergence & Dynamics of Coherent Structures* (Oxford University Press, Oxford, 1999)
2. T. Dauxois, M. Peyrard, *Physics of Solitons* (Cambridge University Press, Cambridge, 2006)
3. R.D. Parmentier, in *Solitons in Action*, ed. by K. Lonngren, A.C. Scott (Academic, New York, 1978), pp. 173–200
4. D.W. McLaughlin, A.C. Scott, Phys. Rev. A **18**, 1652 (1978)

5. A. Barone, G. Paternò, *Physics and Applications of the Josephson Effect* (Wiley, New York, 1982)
6. N.F. Pedersen, in *Solitons*, ed. by S.E. Trullinger, V.E. Zakharov, V.L. Pokrovsky (Elsevier, Amsterdam, 1986), pp. 469–502
7. R.D. Parmentier, in *The New Superconducting Electronics*, ed. by H. Weinstock, R.W. Ralston (Springer, Berlin, 1993), pp. 221–245; and arXiv:patt-sol/9303003
8. A.V. Ustinov, Physica D **123**, 315 (1998)
9. B.D. Josephson, Phys. Lett. **1**, 251 (1962)
10. J.R. Waldram, Rep. Prog. Phys. **39**, 751 (1976)
11. K.K. Likharev, *Dynamics of Josephson Junctions and Circuits* (Gordon and Breach Science, 1984)
12. T.P. Orlando, K.A. Delin, *Foundations of Applied Superconductivity* (Addison Wesley, Reading, 1991)
13. M. Tinkham, *Introduction to Superconductivity* (McGraw–Hill, New York, 1996)
14. W.C. Stewart, Appl. Phys. Lett. **12**, 277 (1968)
15. D.E. McCumber, J. Appl. Phys. **39**, 3113 (1968)
16. A.C. Scott, F.Y.F. Chu, S.A. Reible, J. Appl. Phys. **47**, 3272 (1976)
17. Y.S. Kivshar, B.A. Malomed, Rev. Mod. Phys. **61**, 800 (1989)
18. A.C. Scott, W.J. Johnson, Appl. Phys. Lett. **14**, 316 (1969)
19. J.T. Chen, T.F. Finnegan, D.N. Langenberg, in *Proceedings of the Internatioanl Conference on Superconductivity*, ed. by F. Chilton (Elsevier, Amsterdam, 1971), p. 413
20. A. Barone, J. Appl. Phys. **42**, 2747 (1971)
21. T.A. Fulton, R.C. Dynes, Solid State Commun. **12**, 57 (1973)
22. A. Davidson, B. Dueholm, B. Kryger, N.F. Pedersen, Phys. Rev. Lett. **55**, 2059 (1985)
23. A. Davidson, B. Dueholm, N.F. Pedersen, J. Appl. Phys. **60**, 1447 (1986)
24. A.V. Ustinov, T. Doderer, R. Huebener, Phys. Rev. Lett. **69**, 1815 (1992)
25. A.V. Ustinov, Appl. Phys. Lett. **80**, 3153 (2002)
26. A. Wallraff, A.V. Ustinov, V. Kurin, I. Shereshevsky, N. Vdovicheva, Phys. Rev. Lett., **84**, 151 (2000)
27. N. Grønbech-Jensen, P.S. Lomdahl, M.R. Samuelsen, Phys. Lett. A **154**, 14 (1991)
28. N. Martucciello, R. Monaco, Phys. Rev. B. **53**, 3471 (1996)
29. A.V. Ustinov, B. Malomed, N. Thyssen, Phys. Lett. A **233**, 239 (1997)
30. A. Wallraff, Y. Koval, M. Levitchev, M.V. Fistul, A.V. Ustinov, J. Low Temp. Phys **118**, 543 (2000)
31. E. Goldobin, A. Sterck, D. Koelle, Phys. Rev. E **63**, 031111 (2001)
32. G. Carapella, G. Costabile, Phys. Rev. Lett. **87**, 077002 (2001)
33. M. Beck, E. Goldobin, M. Neuhaus, M. Siegel, R. Kleiner, D. Koelle, Phys. Rev. Lett. **95**, 090603 (2005)
34. H.B. Wang, B.Y. Zhu, C. Gürlich, M. Ruoff, S. Kim, T. Hatano, B.R. Zhao, Z.X. Zhao, E. Goldobin, D. Koelle, R. Kleiner, Phys. Rev. B **80**, 224507 (2009)
35. S. Sakai, P. Bodin, N.F. Pedersen, J. Appl. Phys. **73**, 2411 (1993)
36. M.B. Mineev, G.S. Mkrtchjan, V.V. Schmidt, J. Low Temp. Phys., **45**, 497 (1981)
37. P.R. Auvil, J.B. Ketterson, J. Appl. Phys. **61** 1957 (1987)
38. A.V. Ustinov, H. Kohlstedt, M. Cirillo, N.F. Pedersen, G. Hallmanns, C. Heiden Phys. Rev. B **48**, 10614 (1993)
39. S. Sakai, A.V. Ustinov, H. Kohlstedt, A. Petraglia, N.F. Pedersen, Phys. Rev. B **50**, 12905 (1994)
40. R. Kleiner, F. Steinmeyer, P. Kunkel, P. Müller, Phys. Rev. Lett. **68**, 2394 (1992)
41. G. Oya, N. Aoyama, A. Irie, S. Kishida, H. Tokutaka, Jpn. J. Appl. Phys. **31**, L829 (1992)
42. R. Kleiner, P. Müller, Phys. Rev. B **49**, 1327 (1994)
43. J.U. Lee, J.E. Nordman, G. Hohenwarter, Appl. Phys. Lett. **67**, 1471 (1995)
44. A. Yurgens, D. Winkler, N. Zavaritsky, T. Claeson, Phys. Rev. B **53**, R8887 (1996)
45. Y.I. Latyshev, J.E. Nevelskaya, P. Monceau, Phys. Rev. Lett. **77**, 932 (1996)

46. G. Hechtfischer, R. Kleiner, K. Schlenga, W. Walkenhorst, P. Müller, H.L. Johnson, Phys. Rev. B **55**, 14638 (1997)
47. V.P. Koshelets, S.V. Shitov, L.V. Filippenko, A.M. Baryshev, W. Luinge, H. Golstein, H. van de Stadt, J.-R. Gao, T. de Graauw, IEEE Trans. Appl. Supercond. **7**, 3589 (1997)
48. M. Tachiki, M. Iizuka, K. Minami, S. Tejima, H. Nakamura, Phys Rev. B **71**, 134515 (2005)
49. S. Savel'ev, A.L. Rakhmanov, V.A. Yampol'skii, F. Nori, Nature Phys. **2**, 521 (2006)
50. L. Ozyuzer, A.E. Koshelev, C. Kurter, N. Gopalsami, Q. Li, M. Tachiki, K. Kadowaki, T. Yamamoto, H. Minami, H. Yamaguchi, T. Tachiki, K.E. Gray, W.-K. Kwok, U. Welp, Science **318**, 1291 (2007)
51. A. Dienst, M.C. Hoffmann, D. Fausti, J.C. Petersen, S. Pyon, T. Takayama, H. Takagi, A. Cavalleri, Nature Photon. **5**, 485 (2011)
52. D.Y. An, J. Yuan, N. Kinev, M.Y. Li, Y. Huang, M. Ji, H. Zhang, Z. L. Sun, L. Kang, B. B. Jin, J. Chen, J. Li, B. Gross, A. Ishii, K. Hirata, T. Hatano, V.P. Koshelets, D. Koelle, R. Kleiner, H.B. Wang, W.W. Xu, P.H. Wu, Appl. Phys. Lett. **102**, 092601 (2013)
53. A. Dienst, E. Casandruc, D. Fausti, L. Zhang, M. Eckstein, M. Hoffmann, V. Khanna, N. Dean, M. Gensch, S. Winnerl, W. Seidel, S. Pyon, T. Takayama, H. Takagi, A. Cavalleri, Nat. Mater. **12**, 535 (2013)
54. U. Welp, K. Kadowaki, R. Kleiner, Nat. Photon. **7**, 702 (2013)
55. J.J. Mazo, in *Energy Localisation and Transfer*, ed. by T. Dauxois, A. Litvak-Hinenzon, R.S. MacKay, A. Spanoudaki. Advanced Series in Nonlinear Dynamics, vol. 22 (World Scientific, River Edge, 2004), pp. 193–246
56. C.A. Hamilton, C.J. Burroughs, S.P. Benz, IEEE Trans. Appl. Supercond. **7**, 3756 (1997)
57. J. Clarke, Proc. IEEE **77**, 1208 (1989)
58. S.T. Ruggiero, D.A. Rudman (eds.), *Superconducting Devices* (Academic, Boston, 1990)
59. D. Koelle, R. Kleiner, F. Ludwig, E. Dantsker, J. Clarke, Rev. Mod. Phys. **71**, 631 (1999)
60. A.V. Ustinov, Chaos **13**, 716 (2003)
61. J.J. Mazo, T.P. Orlando, Chaos **13**, 733 (2003)
62. R.S. Newrock, C.J. Lobb, U. Geigenmüller, M. Octavio, Solid State Phys. **54**, 263 (2000)
63. L.M. Floría, J.J. Mazo, Adv. Phys. **45** 505 (1996)
64. O. Braun, Yu.S. Kivshar, Phys. Rep. **306**, 1 (1998)
65. O. Braun, Yu.S. Kivshar, *The Frenkel-Kontorova Model. Concepts, Methods and Applications* (Springer, Berlin, 2004)
66. A.V. Ustinov, M. Cirillo, B.A. Malomed, Phys. Rev. B **47**, 8357 (1993)
67. S. Watanabe, H.S.J. van der Zant, S.H. Strogatz, T.P. Orlando, Physica D **97**, 429 (1996)
68. F. Falo, P.J. Martínez, J.J. Mazo, S. Cilla, Europhys. Lett. **45**, 700 (1999)
69. E. Trías, J.J. Mazo, F. Falo, T.P. Orlando, Phys. Rev. E **61**, 2257 (2000)
70. F. Falo, P.J. Martínez, J.J. Mazo, T.P. Orlando, K. Segall, E. Trías, Appl. Phys. A **75**, 263 (2002)
71. J. Pfeiffer, M. Schuster, A.A. Abdulmalikov Jr., A.V. Ustinov, Phys. Rev. Lett. **96**, 034103 (2006)
72. A.J. Sievers, S. Takeno, Phys. Rev. Lett. **61**, 970 (1988)
73. S. Flach, C.R. Willis, Phys. Rep. **295**, 181 (1998)
74. Focus Issue on "Nonlinear localized modes: physics and applications". Chaos **13**(2) (2003)
75. S. Flach, A.V. Gorbach, Phys. Rep. **467**, 1 (2008)
76. E. Trías, J.J. Mazo, T.P. Orlando, Phys. Rev. Lett. **84**, 741 (2000)
77. P. Binder, D. Abraimov, A.V. Ustinov, S. Flach, Y. Zolotaryuk, Phys. Rev. Lett. **84**, 745 (2000)
78. E. Trías, J.J. Mazo, T.P. Orlando, Phys. Rev. B **65**, 054517 (2002)
79. J. Clarke, A.N. Cleland, M.H. Devoret, D. Esteve, J.M. Martinis, Science **239**, 992 (1988)
80. I. Georgescu, F. Nori, Phys. World **25**, 16 (2012)
81. J. Clarke, F.K. Wilhelm, Nature **453**, 1031 (2008)
82. J.Q. You, F. Nori, Nature **474**, 589 (2011)
83. M.H. Devoret, R.J. Schoelkopf, Science **339**, 1169 (2013)
84. A. Wallraff, A. Lukashenko, J. Lisenfeld, A. Kemp, M.V. Fistul, Y. Koval, A.V. Ustinov, Nature **425**, 155 (2003)

85. M.V. Fistul, A. Wallraff, Y. Koval, A. Lukashenko, B.A. Malomed, A.V. Ustinov, Phys. Rev. Lett. **91**, 257004 (2003)
86. A.N. Price, A. Kemp, D.R. Gulevich, F.V. Kusmartsev, A.V. Ustinov, Phys. Rev. B **81**, 014506 (2010)
87. K.G. Fedorov, A.V. Shcherbakova, M.J. Wolf, D. Beckmann, A.V. Ustinov. Phys. Rev. Lett. **112**, 160502 (2014)
88. K.G. Fedorov, A.V. Shcherbakova, R. Schäfer, A.V. Ustinov, Appl. Phys. Lett. **102**, 132602 (2013)
89. E. Goldobin, K. Vogel, O. Crasser, R. Walser, W. Schleich, D. Koelle, R. Kleiner, Phys. Rev. B **72**, 054527 (2005)
90. M. Weides, M. Kemmler, H. Kohlstedt, R. Waser, D. Koelle, R. Kleiner, E. Goldobin, Phys. Rev. Lett. **97**, 247001 (2006)
91. K. Cedergren, J.R. Kirtley, T. Bauch, G. Rotoli, A. Troeman, H. Hilgenkamp, F. Tafuri, F. Lombardi, Phys. Rev. Lett. **104**, 177003 (2010)
92. S. Scharinger, M. Turad, A. Stöhr, V. Leca, E. Goldobin, R.G. Mints, D. Koelle, R. Kleiner, Phys. Rev. B **86**, 144531 (2012)
93. H. Sickinger, A. Lipman, M. Weides, R.G. Mints, H. Kohlstedt, D. Koelle, R. Kleiner, E. Goldobin, Phys. Rev. Lett. **109**, 107002 (2012)
94. E. Goldobin, R. Kleiner, D. Koelle, Phys. Rev. B **87**, 224501 (2012)
95. D.M. Heim, K. Vogel, W.P. Schleich, D. Koelle, R. Kleiner, E. Goldobin, New J. Phys. **15**, 053020 (2013)
96. T. Fulton, R. Dynes, P.W. Anderson, Proc. IEEE **61**, 28 (1973)
97. K.K. Likharev, in *The New Superconducting Electronics*, ed. by H. Weinstock, R.W. Ralston (Springer, Berlin, 1993), pp. 423–452
98. K.K. Likharev, V.K. Semenov, A. Zorin, in *Superconducting Devices*, ed. by S.T. Ruggiero, D.A. Rudman (Academic, Boston, 1990), pp. 1–49
99. P. Bunyk, K.K. Likharev, D. Zinoviev, Int. J. High Speed Electron. **11**, 257 (2001)
100. V.K. Semenov, G.V. Danilov, D.V. Averin, IEEE Trans. Appl. Supercond. **13**, 938 (2003)
101. V.K. Semenov, G.V. Danilov, D.V. Averin, IEEE Trans. Appl. Supercond. **17**, 938 (2007)
102. J. Ren, V.K. Semenov, IEEE Trans. Appl. Supercond. **21**, 780 (2011)
103. K.K. Likharev, Physica C **482**, 6 (2012)